International Journal of Food Science +Technology

Institute of Food Science +Technology ifst

International Journal of Food Science and Technology 2024, **59**, 1709–1723

Original article

Fabrication and characterisation of Pickering emulsion-based oleogel stabilised by citrus fibre and whey protein isolate colloidal complex: application in cookie formulation

Ezgi Genc,[1] Salih Karasu,[2]* Alican Akcicek[3] & Omer Said Toker[2]

1 Department of Food Quality Control and Analysis, Vocational School of Health Services, İstanbul Gelişim University, Istanbul 34210, Turkey
2 Department of Food Engineering, Faculty of Chemical and Metallurgical Engineering, Yildiz Technical University, Davutpasa Campus, Istanbul 34210, Turkey
3 Faculty of Tourism Department of Gastronomy and Culinary Arts, Kocaeli University, Kartepe, Kocaeli 41080, Turkey

(Received 13 September 2023; Accepted in revised form 2 January 2024)

Summary In this study, the oleogel was produced by Pickering emulsion-based method by using citrus fibre (*CF*)-whey protein isolate (WPI) colloidal complex. The obtained oleogels were characterised by rheological and textural properties, and then the oleogels were used in cookies as an alternative to palm oil. The four oleogels (1% to 5%) were fabricated using a *CF*-10% WPI complex. Shear thinning rheological behaviour was observed in all emulsion and oleogel samples. The *G* values were greater than the *G* values, indicating that solid-like behaviour dominated in all emulsion and oleogel samples. All oleogel samples had a higher than 90% oil-holding capacity. The visual appearance of 3% *CF*-10% WPI and 5% *CF*-10% WPI showed no surface oil, and more integrity structure means that could well trap oil in a gel matrix. Increasing CF% concentration reduced oil droplets and created a more compact structure, particularly at 3% and 5% CF-10% WPI. An increase in *CF* concentration from 2% to 5% led to an increase in the hardness value of the dried products and cookies that *CF* formed a 3D network structure with binds liquid oil. The oxidative stability showed that no significant changes were found between the 3% *CF*-10% WPI and palm cookies ($P < 0.05$). Cookies containing oleogels with a 3% *CF* content exhibited a visual resemblance to this trait, suggesting a colour appearance that closely resembled cookies made with palm oil. The incorporation of oleogels into the cookie recipe proved to be an effective substitute for palm oil. *CF*-10% WPI oleogels show promise for use in cookie preparation as a replacement for palm oil, offering potential as substitutes for saturated and trans fats in food products.

Keywords Citrus fibre, emulsion templated, oleogel, palm oil, whey protein isolate.

Introduction

The food industry commonly uses saturated and trans fats for their ability to enhance texture, mouthfeel and flavour, but their widespread consumption has been linked to several adverse health effects, including cardiovascular disease, inflammation, oxidative stress and endothelial dysfunction (Qiu *et al.*, 2018; Martins *et al.*, 2020). There is a need to develop new methods that can transform liquid oils into solid fats without creating trans fatty acids and lower levels of saturated fatty acids to protect consumer health. Oleogelation, a technology created by structuring agents, is regarded as a viable solution to the problem because it entails gelling oil and lowering the amount of trans-free and saturated fat (Manzoor *et al.*, 2022).

Oleogels are solid-like substances that entrap oil within a three-dimensional network formed by structuring molecules (Plazzotta *et al.*, 2020). Despite the identification of several oil gelators, many of them are liposoluble molecules (such as wax and wax esters, ethylcellulose, phytosterols and fatty acid derivatives) that are frequently restricted in food use (Martins *et al.*, 2020).

Typically, oleogels are created by adding oleogelators (such as beeswax, monoglyceride and ethyl cellulose) directly to liquid oil. The dispersed oleogelators can then self-assemble into stable networks, resulting in a solid-like gel structure (Brito *et al.*, 2022; Li *et al.*, 2023a). However, the choices for selecting oleogelators

*Correspondent: E-mail: skarasu@yildiz.edu.tr

doi:10.1111/ijfs.16925
© 2024 The Authors. *International Journal of Food Science & Technology* published by John Wiley & Sons Ltd on behalf of Institute of Food, Science and Technology (IFSTTF).
This is an open access article under the terms of the Creative Commons Attribution License, which permits use, distribution and reproduction in any medium, provided the original work is properly cited.

are restricted because they must be soluble in oil. Recently, there has been an increasing interest in oleogels produced from emulsions, which are particularly interesting due to their organised network and capacity to replace trans fats (Li *et al*., 2023a). Creating oleogels through emulsions that use food-grade polymers is a viable option for substituting saturated and trans fats (Espert *et al*., 2022). Citrus peel, which is a by-product of the citrus consumption process, is a major source of natural plant-based dietary fibres. These fibres are obtained from the pectin extraction process from citrus peel. Natural citrus dietary fibres are primarily composed of carbohydrates, including cellulose, hemicellulose, pectin and some oligosaccharides. They may also contain small amounts of fat, protein and ash. Citrus fibres have been used in various applications due to their multiple functionalities, such as water retention, emulsification and gelling. They are widely used to enhance the texture, nutrition, cost and labelling of foods (Chen *et al*., 2023). Citrus fibres have been utilised to enhance the texture and stability of emulsified food systems (Chatsisvili *et al*., 2012; Ruan *et al*., 2019).

Whey protein isolate is a natural protein that can be sourced widely and is highly compatible and degradable. It also can create gels under specific conditions, making it a superior option for producing food-grade aerogels (Zhao *et al*., 2023).

This study aimed to investigate the stabilising effects of *CF*-WPI complexes on oleogels and applied in cookie products. The objective was to elucidate the structural properties and stabilising mechanisms of these colloidal complexes in oleogels and provide practical information for creating oleogels with improved physicochemical stability using natural materials. The potential of *CF*-WPI-stabilised oleogels as a palm oil alternative was investigated. Various characteristics including texture, colour properties and oxidative stability of the cookies made with oleogels were analysed. The findings provide useful information development of *CF*-WPI-stabilised oleogels and their utilisation in the food industry.

Materials and methods

Materials

In this study, the extra virgin olive oil used as the oil phase, palm oil, wheat flour, sucrose, wheat starch, baking powder and salt were obtained from local markets in Turkey. WPI was obtained from Hardline Nutrition (Bionet Food Cosmetics Ind. Domestic and Foreign Trade Marketing Joint Stock Company-Kocaeli, Turkey). *CF* was obtained from CP Kelco Company (Limeira, Brazil). All chemical materials and standards were purchased by Sigma Chem. Co. (St. Louis, MO, USA) and Merck (Darmstadt, Germany).

Preparation of colloidal complex, emulsion and oleogels

Oleogels were produced according to the modified method (Qiu *et al*., 2018). In the oleogel formulation, a colloidal complex (CC) was formed by dissolving whey protein (10%) and citrus fibre (1%–5%) in water. Then, (CC) (55%) and olive oil (45%) were homogenised in an ULTRA-TURRAX homogeniser (IKA-Works Inc.) at 2742 *g* for 3 min. The resulting emulsions were dried in a freeze dryer (Martin Christ, Beta 1–8 LSC plus, Osterode am Harz, Germany) at −55 °C, 1 hPa pressure, for 72 h. The oleogels were produced after the dried samples from the freeze dryer were shredded for 20 s using a house-type coffee grinder (Kiwi-KSPG-4812). The oleogels were stored at +4 °C until the analysis period.

Rheological properties

All rheological properties of the emulsion and oleogel samples were determined using a rheometer (MCR 302; Anton Paar, Austria) with a stress- and temperature-controlled Peltier heating system. The rheological analyses were conducted in triplicate at 25 °C.

The flow behaviour in the rheological properties of the samples was determined in the range of 0–100 s^{-1} shear rate using a parallel plate configuration and a 0.5 mm gap between the rheometer probe and the sample plate. Shear stress and apparent viscosity values corresponding to shear rate were recorded. The parameters of the flow behaviour rheological properties were calculated using the Power law model and nonlinear regression.

$$\tau = K \times \gamma^n \tag{1}$$

The τ value specified in the formula is the shear stress (Pa), K is the consistency coefficient (Pa.s^n), γ is the shear rate (s^{-1}) and n is the flow behaviour index.

Dynamic rheological analysis of the emulsion and oleogel samples was performed with parallel plate configuration. First, the amplitude sweep test was performed with a strain value of 0.1% to determine the linear viscoelastic region (LVR). A frequency sweep test was applied in the frequency range of 0.1–10 Hz. The storage modulus (G') and loss modulus (G'') were determined depending on the angular velocities of the samples. Power law model and nonlinear regression were used to calculate dynamic rheological parameters (Yoo & Rao, 1996).

$$G' = K'(\omega)^{n'} \tag{2}$$

$$G'' = K''(\omega)^{n''} \tag{3}$$

The G' value specified in the formula is the storage modulus (Pa), the G'' value is the loss modulus (Pa), ? is the angular velocity value (s^{-1}), K', K'' are the

 © 2024 The Authors. *International Journal of Food Science & Technology* published by John Wiley & Sons Ltd on behalf of Institute of Food, Science and Technology (IFSTTF).

13652621, 2024, 3, Downloaded from https://ifst.onlinelibrary.wiley.com/doi/10.1111/ijfs.16925 by Istanbul Gelisim Universitesi, Wiley Online Library on [14/02/2024]. See the Terms and Conditions (https://onlinelibrary.wiley.com/terms-and-conditions) on Wiley Online Library for rules of use; OA articles are governed by the applicable Creative Commons License

13652621, 2024, 3, Downloaded from https://ifst.onlinelibrary.wiley.com/doi/10.1111/ijfs.16925 by Istanbul Gelisim Universitesi, Wiley Online Library on [14/02/2024]. See the Terms and Conditions (https://onlinelibrary.wiley.com/terms-and-conditions) on Wiley Online Library for rules of use; OA articles are governed by the applicable Creative Commons License

consistency coefficient values (Pas^n) and n', n'' are flow behaviour index values.

The samples were subjected to the three-interval thixotropy test (3-ITT) to determine the level of recovery resulting from high deformation. The measurements of 3-ITT method were conducted at two different shear rates: a constant rate of 0.5 s^{-1} and a variable rate of 150 s^{-1}. After thorough consideration, the LVR was determined to be 50 s^{-1} when selecting the values. The samples underwent a low shear rate of 0.5 s^{-1} for 100 s in the first interval, followed by a high shear rate of 150 s^{-1} for 40 s in the second interval. During the third interval, the samples were subjected to the same shear rate as was delivered during the first interval, and their ability to recover was evaluated. To achieve this objective, the alteration in the G' value was documented.

A temperature sweep test was conducted to analyse the temperature-dependent characteristics of the oleogel samples. The variations in the G' value of the samples were analysed within the temperature range of 20 °C to 80 °C. The temperature was raised by 5 °C for a duration of 1 min.

FTIR

A Bruker Tensor 27 spectrometer (Bremen-Germany) equipped with an ATR accessory with a diamond crystal module was used in this study. The detector was a DLaTGS detector with a KBr beam splitter. OPUS program Version 7.2 for Windows from Bruker Gmbh was used for instrument control and data acquisition. Infrared spectra were recorded in the wavelength range from 3800 to 600 cm^{-1} at 4 cm^{-1} resolution, accumulating 64 scans per spectra. The whey protein and citrus fibre powder, olive oil, dried products and oleogel samples were analysed by FTIR (Ozulku *et al.*, 2017).

Oil-holding capacity

The oil-holding capacity of oleogel samples was determined according to the study by Xie *et al.* (2023). Accordingly, oleogel samples were weighed into a 10 mL centrifuge tube and their weights were recorded (m_0). Tubes were centrifuged at 1147 ***g*** for 10 min. After centrifugation, the precipitate was discarded and the weight of the tube was recorded as m_1. The oil-holding capacity was calculated using the following equation:

$$\text{Oil}-\text{holding capacity}\ (\%) = m_1/m_0 \times 100 \qquad (4)$$

Preparation of cookies

The study conducted by Yılmaz & Öğütcü (2015) was utilised for the modification of cookie compositions. To begin with, the conventional cookie mix was produced, consisting of 65% wheat flour, 19% sucrose, 11% maltodextrin, 3.5% wheat starch, 0.5% baking powder and 1% salt. Following that, a mixture was created using 67.76% cookie mix, 23.69% oil phase (consisting of palm oil, oleogel containing 3% and 5% *CF*) and 8.55% homogenised egg to generate the cookie dough by mixing with a kitchen mixer (Kitchen Aid, Stand Mixer – 5K45SS, Michigan, USA) for 5 min at medium speed. The dough was rolled up by hand, thinned to 1 cm width, and shaped by cutting with a 5-cm-diameter round stainless steel cookie cutter. Cookies were baked at 170 °C for 15 min and cooled to room temperature. The Cookie samples were then analysed.

Visual appearance and microscopy

The emulsions, dried products, oleogel samples, cookie dough and cookie samples photographs were taken with a smartphone (iPhone 13) camera. The samples were examined under a polarised light microscope (Olympus BX41, Tokyo, Japan) that had a digital camera for microscopic analysis. A tiny amount of oleogel was placed on a slide and covered with a cover slip. Subsequently, images of the samples were captured using a 40× magnification.

Texture profile analysis

The hardness, chewiness and cohesiveness of freeze-dried emulsion and cookie samples were evaluated using a texture analyser (TA.XT2 Plus, Godalming, UK). A penetration test was carried out on the freeze-dried emulsion samples and cookies with the use of a needle probe. The samples were positioned immediately between a cylindrical probe of 40 mm diameter and the metal plate. The penetration depth of the dried samples was set at 10 mm at a rate of 1 mm/s with a 5 *g* trigger force. The compression examination of the materials was conducted using a cylinder probe with a diameter of 4 mm. The velocity of the probe for the compression test was set to 1.0 mm s^{-1}. The time interval between two bites was set at 5.0 s, the trig force was 2 grammes and the compression ratio was set at 65%. The hardness, consistency and adhesion properties were quantified (Giacintucci *et al.*, 2018; Qiu *et al.*, 2018).

Oxidative stability of cookies

The oxidative stability of the cookie samples was determined using the OXITEST instrument (Velp Scientifica, Usmate, MB, Italy). First of all, the cookie samples were ground in a household coffee grinder (Kiwi-KSPG-4812) for 5 s. Then, each sample was

© 2024 The Authors. *International Journal of Food Science & Technology* published by John Wiley & Sons Ltd on behalf of Institute of Food, Science and Technology (IFSTTF).

weighed into the sample cells of the device as 20 grammes. The weighed samples were homogeneously distributed in the sample cell. The samples were analysed at 6 bar oxygen pressure and 90 °C. The oxidative stability values of the samples were interpreted according to the induction period (IP) data obtained from the OXITEST instrument (Akcicek *et al.*, 2021).

Colour properties of cookies

The colour properties of cookie samples were determined by using the PCE-CSM4 Colorimeter (Mark-10, Copiague, NY). Colour analysis from the cookie surfaces was carried out by measuring from three different points of each cookie (Yılmaz & Öğütcü, 2015).

Chroma, hue angle and ΔE were calculated by using a and b values with an Excel package program according to the following formulas:

$$\text{Chroma} = \sqrt{a^2 + b^2} \tag{5}$$

$$\begin{aligned} \text{Hue}(h^\circ) &= \text{ArcTan}(b^*/a^*) \text{ or} \\ \text{Hue}(h^\circ) &= 180 + \text{ArcTan}(b^*/a^*) \end{aligned} \tag{6}$$

$$\Delta E = \sqrt{((\overline{L}_0 - L_1)^2 + (a_0 - a_1)^2 + (b_0 - b_1)^2)s} \tag{7}$$

Sensory properties of cookies

Ten trained panellists, aged between 20 and 30, participated in the sensory analysis. The panellists were first briefed on the cookies' appearance, flavour, texture, colour, crispness and overall acceptance. After that, the panellists were asked to rate these attributes on a 5-point numerical scale (1 being extremely poor, and 5 being very good). The panellists were shown the encrypted samples using various codes. Panellists swished water in their mouths while they alternated between samples (Li *et al.*, 2021).

Statistical analysis

The SPSS 15.0 package program was used to perform statistical analysis on the obtained data. Using the analysis of variance technique (ANOVA), the difference between the group means was determined ($P < 0.05$) and the difference was determined by the Duncan multiple-comparison test.

Results and discussion

Rheological properties of emulsions

The effects of *CF* and WPI on the steady shear, dynamic and 3-ITT rheological properties of emulsions were investigated (Qiu *et al.*, 2018). According to steady shear test (Fig. 1), all emulsion samples showed shear thinning behaviour which means that increasing shear rate led to a decrease in viscosity (Qiu *et al.*, 2018; Espert *et al.*, 2022). Similar results were reported by Huang *et al.*, (2023) and Li *et al.* (2023b). Shear thinning refers to the rearrangement of molecules into the flow structure caused by the disruption of the emulsion matrix during shearing. (Alizadeh *et al.*, 2019; Huang *et al.*, 2023). Emulsion droplets may have formed a network due to their close interaction. Then, increasing shear rates might fracture this network and cause viscosity to decrease (Jiang *et al.*, 2018; Huang *et al.*, 2023).

The flow behaviour parameters were modelled by the power law model ($R^2 > 0.99$). The fitting parameters are given in Table 1. The increase in *CF* concentration of emulsions showed a higher K value with a low n value. An increase in *CF* concentration caused higher viscosity which means that *CF* interacted with water and showed a stronger thickening ability (Huang *et al.*, 2023). As mentioned above, the viscosity depends on the *CF* concentration so the 5% *CF*-WPI K value was found higher than the other emulsion samples.

Figure 1 displayed the G' and G'' values as a function of frequency. All emulsion samples of G' were found higher than the G''. This result could be explained that viscous behaviour was dominated by the elastic behaviour indicating that firm gel-like network structure (Espert *et al.*, 2022; Huang *et al.*, 2023). The presence of *CF* led to an increase in G' and G'' values by increasing *CF* amount. This finding showed that *CF* caused an important change in the viscoelastic properties of the emulsions. Similar results were reported by Xie *et al.* (2023) for tamarind seed polysaccharide (TSP) content. Moreover, progressive increase in G' by increasing frequency provides a characteristic strength gel with a non-covalent crosslink network (Chen *et al.*, 2023).

The power law model results are given in Table 1. The power law parameters were also used to determine the dependence of both moduli on frequency. The R^2 values were found to be >0.99. All oleogels showed high mechanical strength with high K' values and displayed weak dependence of G' on the frequency. Similar results were reported by Espert *et al.* (2022). The weak dependency of G' and G'' values signified that rheological analysis of the emulsions was not importantly affected by the applied low deformation rate. This result is comparable with oleogels which were formed by the emulsion-templated method (Chen *et al.*, 2017; Tavernier *et al.*, 2017; Qiu *et al.*, 2018). The K' values were higher than the K'' values at all concentrations which is consistent with G' and G'' values of emulsions.

The 3-ITT test provides information about the structure recovery characteristics by time-dependent samples. The emulsion samples of the 3-ITT graphic are given in Fig. 2. As mentioned above, the emulsion

 © 2024 The Authors. *International Journal of Food Science & Technology* published by John Wiley & Sons Ltd on behalf of Institute of Food, Science and Technology (IFSTTF).

13652621, 2024, 3, Downloaded from https://ifst.onlinelibrary.wiley.com/doi/10.1111/ijfs.16925 by Istanbul Gelisim Universitesi, Wiley Online Library on [14/02/2024]. See the Terms and Conditions (https://onlinelibrary.wiley.com/terms-and-conditions) on Wiley Online Library for rules of use; OA articles are governed by the applicable Creative Commons License

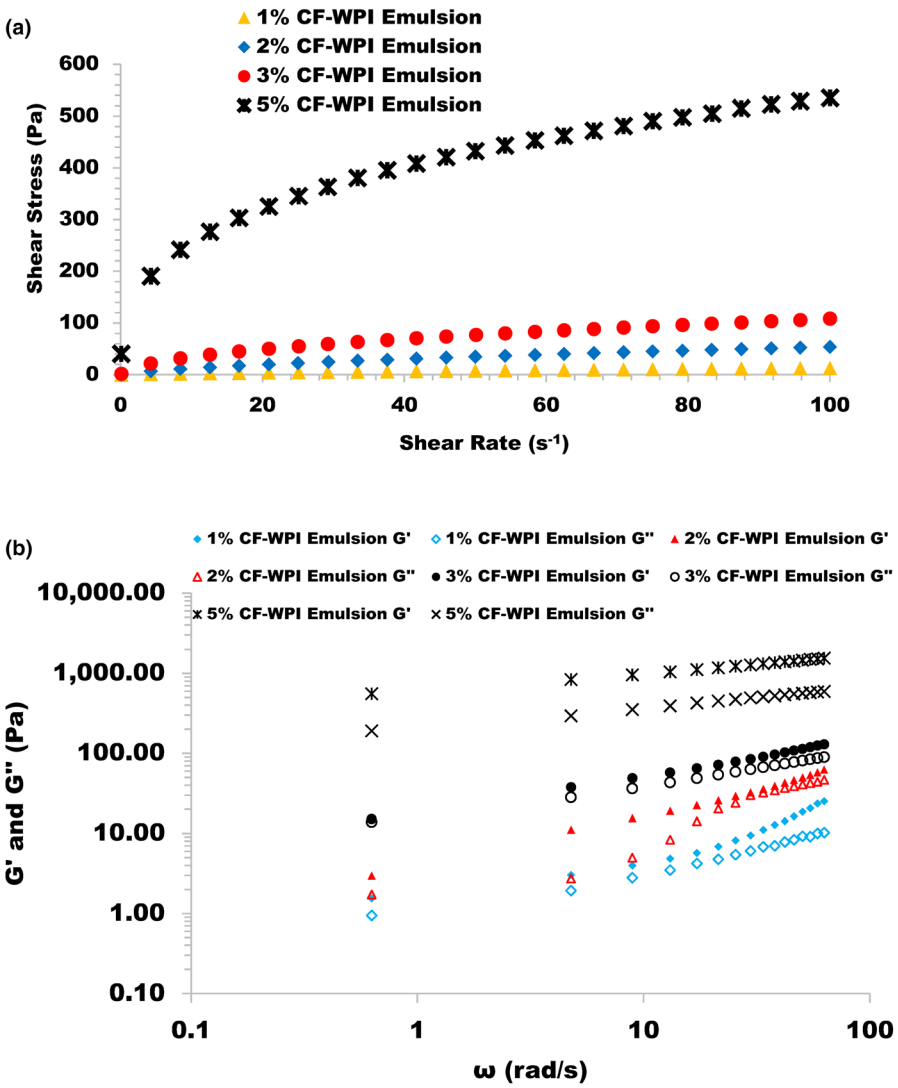


Figure 1 Steady shear (a) and dynamic rheological (b) properties of the emulsions.

samples exhibited shear-thinning behavior, and the viscosity demonstrated a dependency on the concentration of % CF. All emulsion samples showed thixotropic recovery and were highly suitable for spreads except 1% *CF*-WPI emulsion. Similar results were obtained by Brito *et al.*, (2022) and Chen *et al.* (2023). The increase in *CF* caused higher recovery properties due to the long flexible fibrils of the *CF*-formed network which interacted in the aqueous phase and led to increasing viscosity (Chen *et al.*, 2023).

Rheological properties of oleogels

Steady shear rheological properties of oleogel

The flow curves of the oleogels are given in Fig. 3. All oleogel samples showed shear thinning behaviour with increasing shear rate led to a decrease in viscosity (Rao, 2010; Espert *et al.*, 2022; Chen *et al.*, 2023). 5% *CF*-WPI oleogels showed more solid character than the others which led to no possible flow. In addition, the viscosity exhibited dependence on the *CF* concentration. This could be by long-chain flexible fibrils which occurred in the interaction between the network structure and interacted strength at the continuous phase (Chen *et al.*, 2023).

Viscoelastic properties of Oleogel

As can be seen in Fig. 3, all oleogel samples of G' values were higher than the G'' values, which means that oleogels showed elastic and solid-like behaviour (Qiu *et al.*, 2018; Brito *et al.*, 2022). Higher G' values indicated more resistance to deformation which assures

© 2024 The Authors. *International Journal of Food Science & Technology* published by John Wiley & Sons Ltd on behalf of Institute of Food, Science and Technology (IFSTTF).

13652621, 2024, 3, Downloaded from https://ifst.onlinelibrary.wiley.com/doi/10.1111/ijfs.16925 by Istanbul Gelisim Universitesi, Wiley Online Library on [14/02/2024]. See the Terms and Conditions (https://onlinelibrary.wiley.com/terms-and-conditions) on Wiley Online Library for rules of use; OA articles are governed by the applicable Creative Commons License

Table 1 Steady shear and dynamic rheological parameters of emulsions

WPI-*CF* emulsion	*K* (Pas^{-1})	*n*	R^2
Steady shear rheological parameters			
1% *CF*-WPI	0.510 ± 0.004	0.706 ± 0.002	0.99
2% *CF*-WPI	3.012 ± 0.077	0.627 ± 0.005	0.99
3% *CF*-WPI	11.255 ± 0.052	0.492 ± 0.0009	0.99
5% *CF*-WPI	120.982 ± 1.536	0.324 ± 0.006	0.99

WPI-*CF* emulsion	*K′*	*n′*	R^2	*K″*	*n″*	R^2
Dynamic rheological parameters						
1% *CF*-WPI	0.990 ± 0.096	1.189 ± 0.126	0.99	0.617 ± 0.095	0.687 ± 0.085	0.99
2% *CF*-WPI	2.564 ± 0.267	0.761 ± 0.0209	0.99	1.442 ± 0.344	0.857 ± 0.061	0.99
3% *CF*-WPI	15.459 ± 0.411	0.509 ± 0.004	0.99	13.542 ± 0.143	0.456 ± 0.0005	0.99
5% *CF*-WPI	577.766 ± 16.168	0.237 ± 0.006	0.99	202.775 ± 2.126	0.261 ± 0.003	0.99

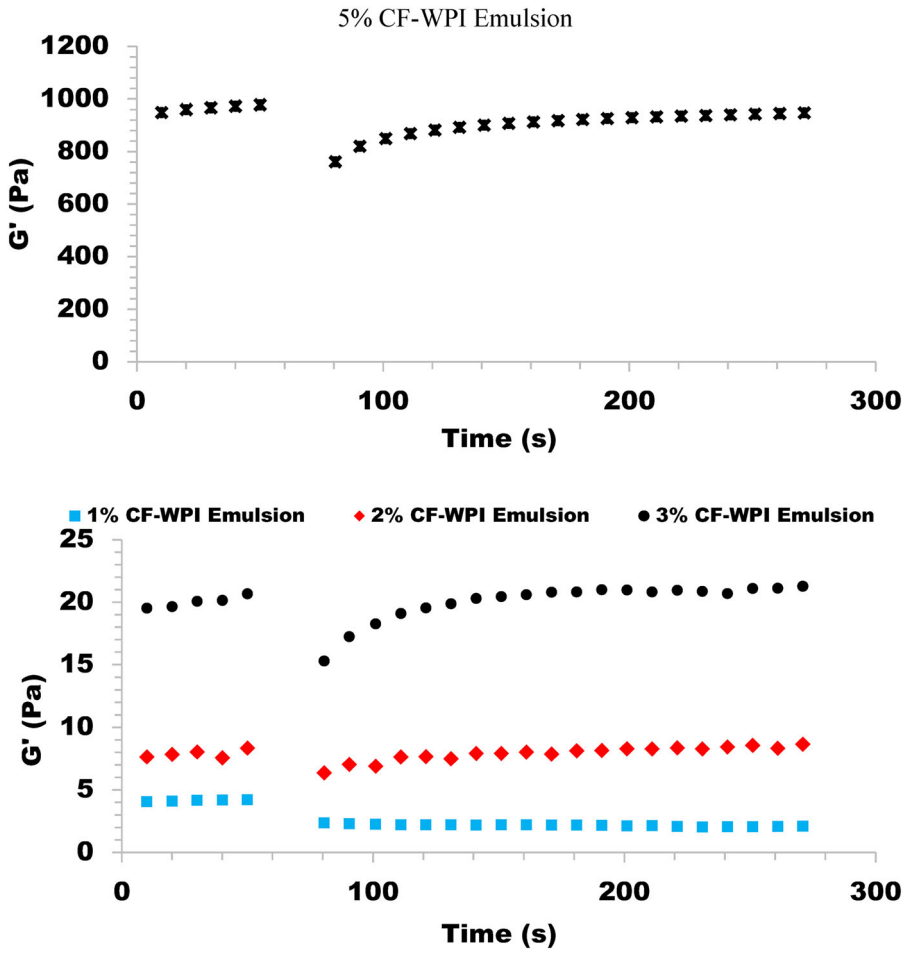


Figure 2 3-ITT rheological properties of emulsion.

more structured material (Chen *et al.*, 2010; Brito *et al.*, 2022). 5% *CF*-WPI showed higher G' values in all oleogel samples. An increase in *CF* concentration resulted in higher G' values (Chen *et al.*, 2023) which found that an increase in the concentration of citrus dietary fibre led to an increase in the values of G' and suggested solid-like behaviour. These results were related to the adsorption and accumulation of WPI

 © 2024 The Authors. *International Journal of Food Science & Technology* published by John Wiley & Sons Ltd on behalf of Institute of Food, Science and Technology (IFSTTF).

13652621, 2024, 3, Downloaded from https://ifst.onlinelibrary.wiley.com/doi/10.1111/ijfs.16925 by Istanbul Gelisim Universitesi, Wiley Online Library on [14/02/2024]. See the Terms and Conditions (https://onlinelibrary.wiley.com/terms-and-conditions) on Wiley Online Library for rules of use; OA articles are governed by the applicable Creative Commons License

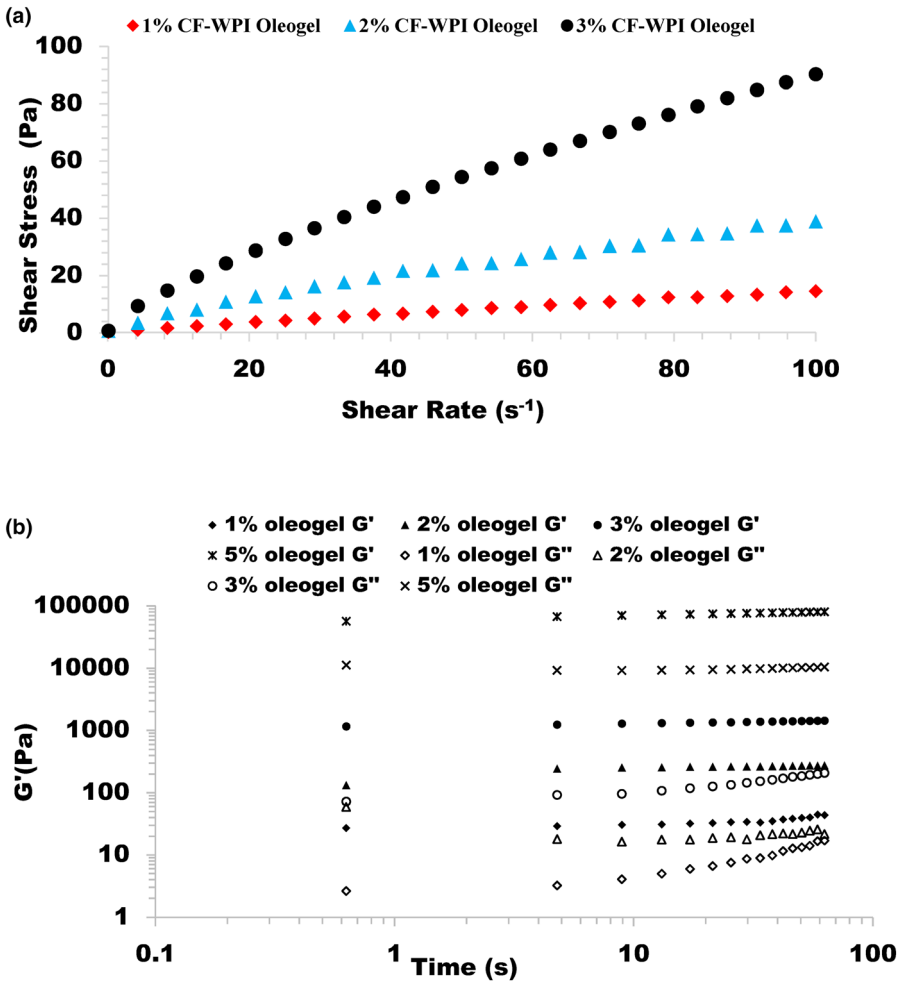


Figure 3 Steady shear (a) and dynamic rheological (b) properties of the oleogels.

and *CF* at the oil–water interface (Song *et al.*, 2022; Chen *et al.*, 2023). In comparison to the moduli values of emulsions and oleogels, G' and G'' values of oleogels were increased after the drying of emulsions led to the creation of a dense cryogel structure (Espert *et al.*, 2022; Xie *et al.*, 2023).

After the water was removed from the emulsion samples, all oleogel samples of G' and viscosity rose due to the interpolymeric network of protein and polysaccharides, resulting in a more compact structure and firmly packed oil droplets. This result could be related to the formation of a bipolymer network at the interface and in the bulk phase at higher concentrations (Wijaya *et al.*, 2019).

Temperature sweep test

Temperature sweep test was conducted on oleogels with different concentrations of *CF* to better understand temperature dependency of the gel structure of these systems and their suitability for use in various food processing. The graphs of G' as a function of temperature are plotted in Fig. 4. From the figure, it is evident that there was a consistent decline in the G' value across all samples as the temperature rose from 20 °C to 80 °C, indicating that gel network of the samples weakened by increasing temperature. The temperature-induced destabilisation of the polymer network may occur due to the disruption of hydrogen bonds, which exhibit reduced strength at elevated temperatures (Davidovich-Pinhas *et al.*, 2015). Other studies have also reported a comparable temperature dependency of the oleogel structure (Davidovich-Pinhas *et al.*, 2015; Hong *et al.*, 2022). From the figure, it is evident that the G' value of the 1% CP-WPI sample experiences a sharp decline after reaching a temperature of 50 °C. This implies that the gel network undergoes a complete collapse as the temperature rises. This outcome indicates that the 1% *CF*-WPI

© 2024 The Authors. *International Journal of Food Science & Technology* published by John Wiley & Sons Ltd on behalf of Institute of Food, Science and Technology (IFSTTF).

13652621, 2024, 3, Downloaded from https://ifst.onlinelibrary.wiley.com/doi/10.1111/ijfs.16925 by Istanbul Gelisim Universitesi, Wiley Online Library on [14/02/2024]. See the Terms and Conditions (https://onlinelibrary.wiley.com/terms-and-conditions) on Wiley Online Library for rules of use; OA articles are governed by the applicable Creative Commons License

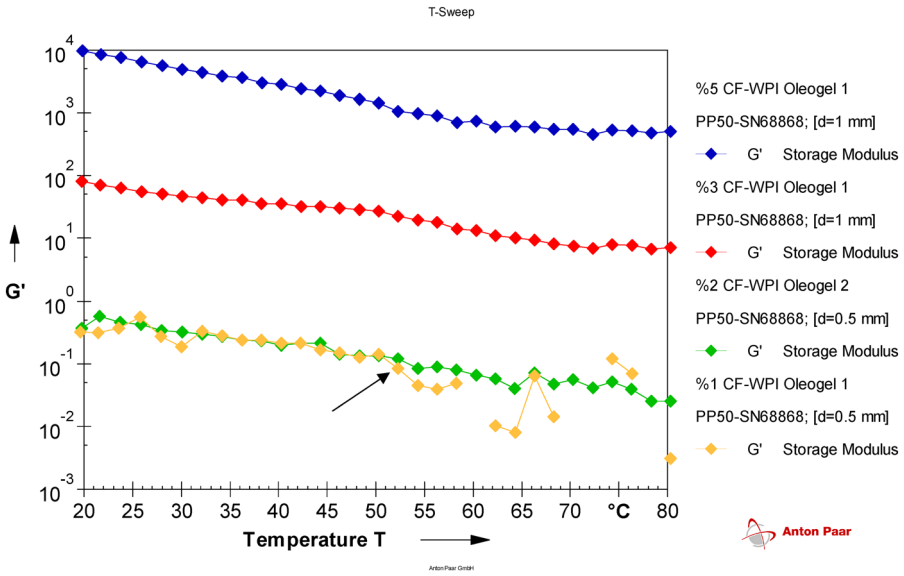


Figure 4 Temperature sweep test of oleogels.

sample is unsuitable for food processes involving high temperatures, whereas other samples may possess thermal resilience.

FTIR

The FTIR spectra were used to ensure information about the interactions of molecules. The FTIR spectra of *CF*, WPI, olive oil and oleogels are given in Fig. 5. The presence of *CF* showed that the structural order of WPI could decrease. This result showed that *CF* could interact with WPI (Qiu *et al.*, 2018). The *CF*-WPI-based oleogel indicated that interaction occurred by Schiff bases at 1634 cm^{-1}, corresponding to the C–N-stretching vibration, an entangled network ability to trap oil (Xu *et al.*, 2018; Brito *et al.*, 2022). Absorption in the wavelength ranges 1600–1700 cm^{-1} is attributed to amide I (CN group between *CF*-WPI). Increasing the concentration of CF from 2% to 5% resulted in OH peaks ranging from 3274 to 3288 cm^{-1}, indicating the formation of intermolecular hydrogen bonding (Shuai *et al.*, 2023). Also, olive oil showed no peak at 3200–3500 cm^{-1}. Polysaccharides contain hydroxyl groups with peaks at 3273 cm^{-1} in *CF* which signified that the hydrogen bonding of oleogels came from polysaccharide (Xu *et al.*, 2023). Hydrogen bonding plays a significant factor in creating a gel network structure (Meng *et al.*, 2018). The creation of hydrogen-bonded polymers led to the semi-crystalline structure of *CF* and WPI so developed the oil entrapment in the polymer matrix (Laredo *et al.*, 2011; Meng *et al.*, 2018; Ma *et al.*, 2023).

The absorption peaks of oleogels at 2922 and 2883 cm^{-1} stretching vibration of C-H from olive oil. The presence of CH bending of CH_3 and CH_2 which is related to citrus fibre and olive oil showed peaks at 1460 and 1461 cm^{-1}. No significant differences were found between the FTIR spectra of the oleogel with different *CF* concentrations except 1% *CF*-WPI oleogels of FTIR spectra.

Oil-holding capacity

The oil-holding capacity (OHC) results are given in Fig. 6. OHC is a significant indicator to assess the compact structure of the oleogels. The sample with the highest %OHC was the 5% *CF*-WPI oleogel with value of 98.90 ± 0.11% OHC. It is followed by 3% *CF*-WPI oleogel (97.64 ± 0.07% OHC), 2% *CF*-WPI oleogel (95.81 ± 0.25% OHC) and 2% *CF*-WPI oleogel (95.54 ± 0.28). All oleogel samples had higher 50% OHC values which means that showed well oil binding and high stability of the oleogel structure (Li *et al.*, 2023a). The increase in *CF* concentration led to higher OHC%. This result explained that *CF* created a 3D network structure in the oleogels which binds to the liquid oil (Shuai *et al.*, 2023). *CF* and WPI could be bound through hydrogen bond interactions, decreasing the oil–water interface tension that improves the stability of oleogels (Chen *et al.*, 2023). Similar results were found by Chen *et al.* (2023). The oil-holding capacity of oleogelators can be correlated with the *G* values and the strong networks with high elasticity increased the oil-holding capacity. The higher

 © 2024 The Authors. *International Journal of Food Science & Technology* published by John Wiley & Sons Ltd on behalf of Institute of Food, Science and Technology (IFSTTF).

13652621, 2024, 3, Downloaded from https://ifst.onlinelibrary.wiley.com/doi/10.1111/ijfs.16925 by Istanbul Gelisim Universitesi, Wiley Online Library on [14/02/2024]. See the Terms and Conditions (https://onlinelibrary.wiley.com/terms-and-conditions) on Wiley Online Library for rules of use; OA articles are governed by the applicable Creative Commons License

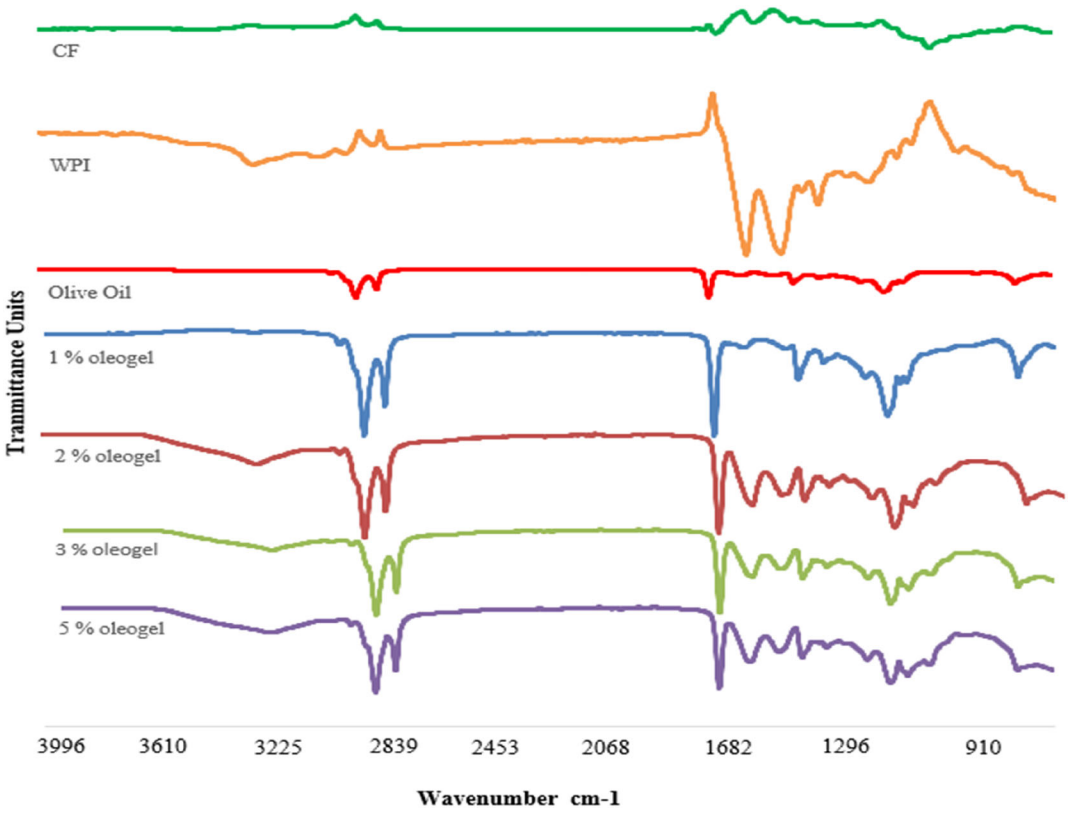


Figure 5 FTIR spectra of the *CF*, WPI, olive oil and oleogels.

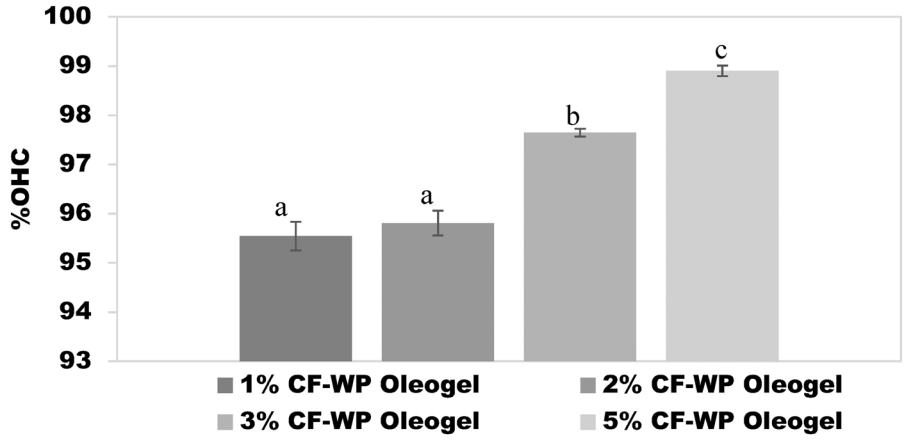


Figure 6 Oil-holding capacity of oleogels. *a-b-c: Different superscript letters indicate significant differences between samples ($p < 0.05$).

G' value was observed in 5% *CF* concentration with higher OHC %. A similar result was found by Jadhav *et al.* (2022). The higher elasticity was found related to the % OHC values of oleogels (da Silva *et al.*, 2019; Li *et al.*, 2023a).

Visual appearance and microstructure properties

Figure 7 shows the photographs of the emulsion, the freeze-dried products and the oleogels. All dried products displayed no surface oil leakage and 3% and 5%

© 2024 The Authors. *International Journal of Food Science & Technology* published by John Wiley & Sons Ltd on behalf of Institute of Food, Science and Technology (IFSTTF).

13652621, 2024, 3, Downloaded from https://ifst.onlinelibrary.wiley.com/doi/10.1111/ijfs.16925 by Istanbul Gelisim Universitesi, Wiley Online Library on [14/02/2024]. See the Terms and Conditions (https://onlinelibrary.wiley.com/terms-and-conditions) on Wiley Online Library for rules of use; OA articles are governed by the applicable Creative Commons License

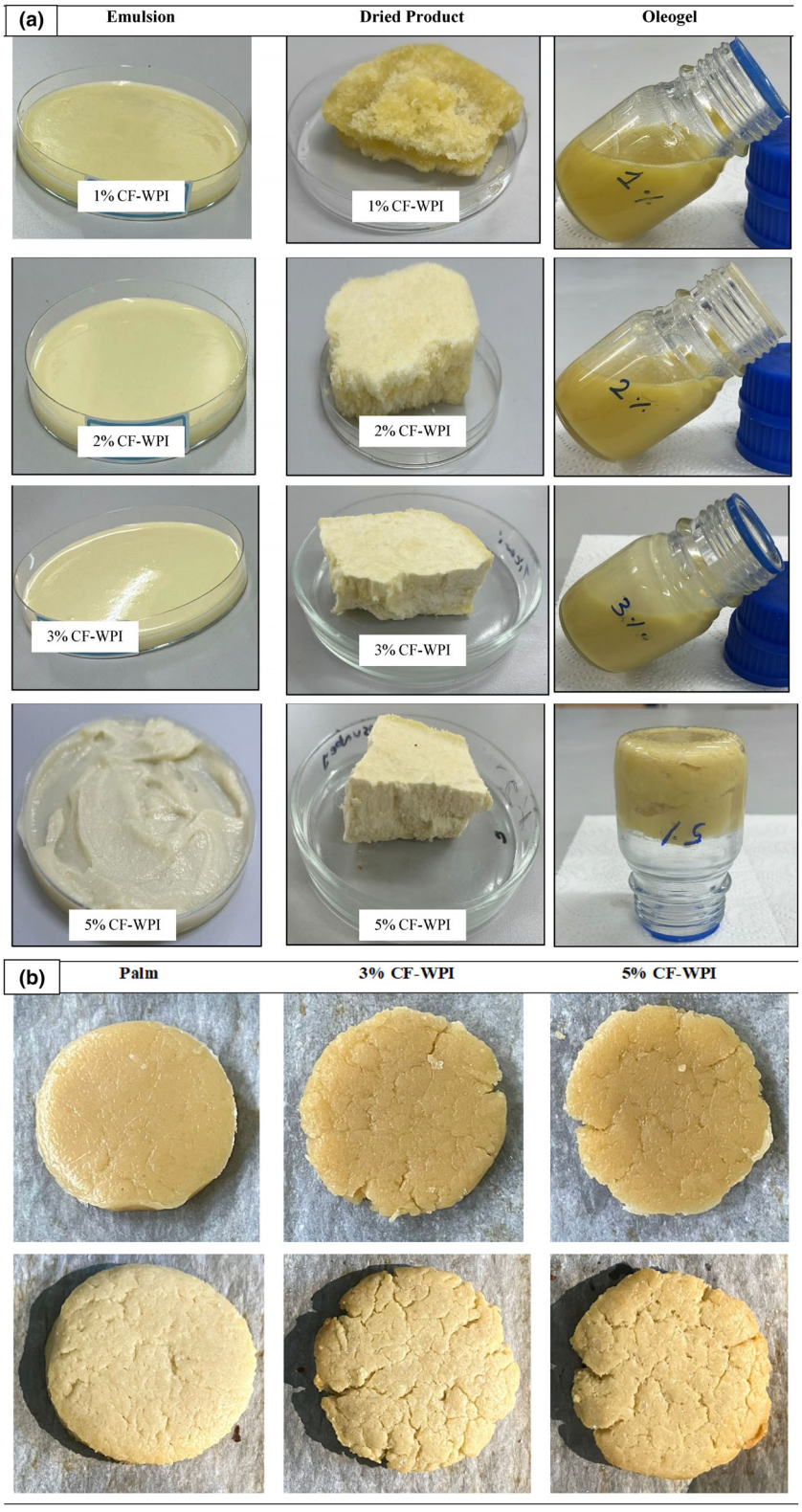


Figure 7 The visual appearance of the emulsion, the freeze-dried products, oleogels, cookie dough and cookies.

 © 2024 The Authors. *International Journal of Food Science & Technology* published by John Wiley & Sons Ltd on behalf of Institute of Food, Science and Technology (IFSTTF).

13652621, 2024, 3, Downloaded from https://ifst.onlinelibrary.wiley.com/doi/10.1111/ijfs.16925 by Istanbul Gelisim Universitesi, Wiley Online Library on [14/02/2024]. See the Terms and Conditions (https://onlinelibrary.wiley.com/terms-and-conditions) on Wiley Online Library for rules of use; OA articles are governed by the applicable Creative Commons License

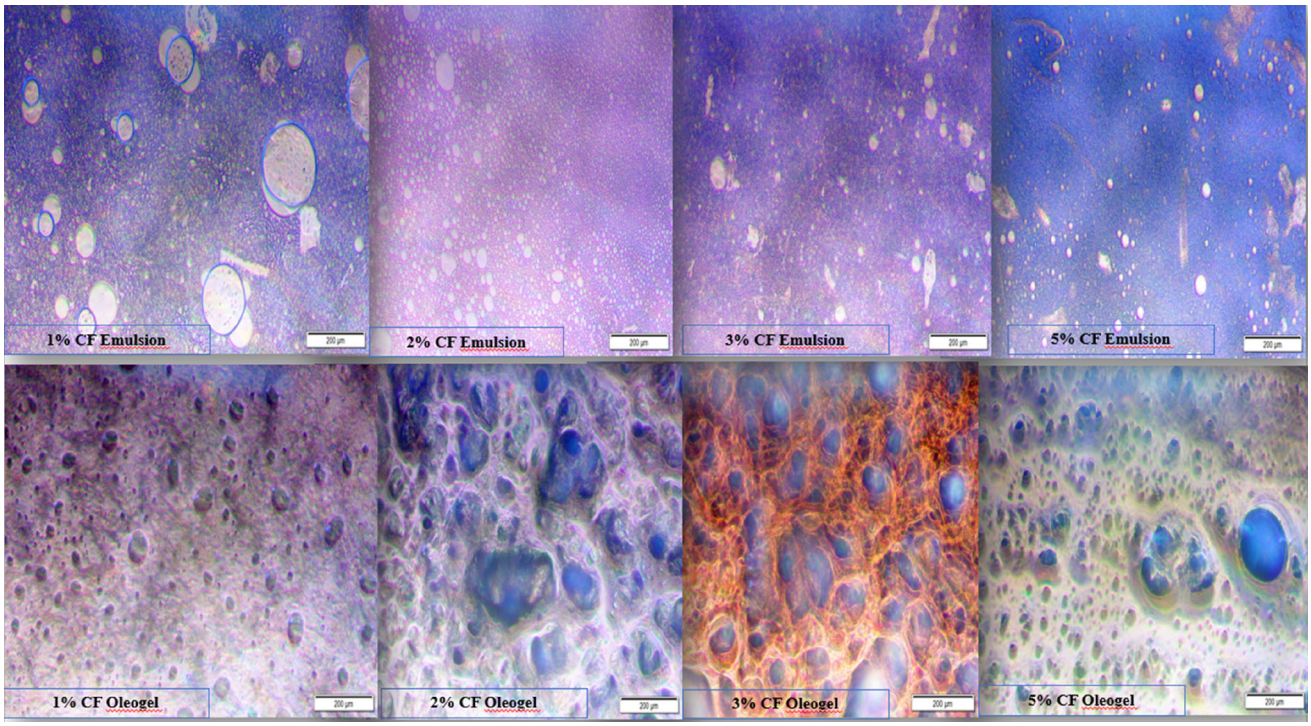


Figure 8 The microstructural properties of the emulsion and oleogels.

CF-WPI showed more integrity structure. This means that the colloidal complex of *CF*-WPI could trap oil in a gel matrix, especially high concentration of *CF* (Qiu *et al*., 2018).

The WPI tends to react with *CF* through hydrogen binding which the WPI is structured by *CF* (Qiu *et al*., 2018; Xie *et al*., 2023). The hydrogen bonding of the colloidal complex improved interfacial structure creation on the oil–water surface. The increase in *CF* concentration provides a strong gel network with densely packed (Qiu *et al*., 2018).

The microstructures of oleogels and emulsions are shown in Fig. 8. An increase in *CF* % concentration led to decreased oil droplets and provided a more compact structure for the emulsions (Huang *et al*., 2023). A higher concentration of the *CF* could increase the viscosity of emulsions. Similar results were reported by Brito *et al*. (2022). This could be explained by that *CF* molecules adsorbed at the droplet interface and reduced the droplet size. A similar result was reported by Huang *et al*. (2023) for the hydroxypropyl methylcellulose molecules. The 1% *CF* of oleogels microstructure displayed packed network with a crystal structure. Nevertheless, this amount of crystals is not enough to provide network structure (Brito *et al*., 2022). In addition, an increase in *CF*% concentration led to form a more compact structure of the oleogels. The higher *CF* could increase the viscosity and the *CF* and WPI complex in the oleogels showed a crosslinked and compact network, especially for 3% and 5% *CF*- WPI. A similar result was reported for the gelatin–tamarind seed polysaccharide (GLT-TSP) complex. (Xie *et al*., 2023). These results showed that CF could bind with WPI through the hydrogen bound. During the drying of the emulsions, the oil droplets are prone to be firmly packed with homogenous distribution in the polymer structure (Brito *et al*., 2022).

Texture profile analysis (dried sample cookies)

The textural properties of dried products and cookies are given in Table 2. As seen in Table 2, increase in *CF* concentration from 2% to 5% led to an increase in hardness value of the dried products from 69.03 to 132.03. Also, the hardness values of cookies showed the same trend. This result explained that *CF* formed a 3D network structure in the dried product which assures strength and binds liquid oil. An increase in the hardness value led to an increase in oil-holding capacity. Similar results were reported by Borriello *et al*. (2021) and Shuai *et al*. (2023). The chewiness value of the dried products increases when the *CF* concentrations increase. However, the chewiness values of cookies decreased when the *CF* concentrations increased.

© 2024 The Authors. *International Journal of Food Science & Technology* published by John Wiley & Sons Ltd on behalf of Institute of Food, Science and Technology (IFSTTF).

13652621, 2024, 3, Downloaded from https://ifst.onlinelibrary.wiley.com/doi/10.1111/ijfs.16925 by Istanbul Gelisim Universitesi, Wiley Online Library on [14/02/2024]. See the Terms and Conditions (https://onlinelibrary.wiley.com/terms-and-conditions) on Wiley Online Library for rules of use; OA articles are governed by the applicable Creative Commons License

Table 2 The texture profile parameters of the dried products and the cookies

Sample	Hardness Dried sample	Chewiness	Cohesiveness
1% *CF*-WPI	ND	ND	ND
2% *CF*-WPI	$69.029^{a} \pm 0.47$	$0.284^{a} \pm 0.026$	$17.543^{a} \pm 1.32$
3% *CF*-WPI	$121.917^{b} \pm 10.44$	$0.302^{a} \pm 0.005$	$22.707^{a} \pm 4.06$
5% *CF*-WPI	$132.034^{b} \pm 9.08$	$0.631^{b} \pm 0.028$	$58.744^{b} \pm 9.16$
Cookies			
Palm	$883.33^{a} \pm 98.09$	$0.161^{b} \pm 0.015$	$127.63^{a} \pm 26.99$
3% *CF*-WPI Oleogel	$1490.75^{b} \pm 120.70$	$0.130^{a} \pm 0.012$	$180.08^{b} \pm 34.55$
5% *CF*-WPI Oleogel	$1935.67^{c} \pm 118.64$	$0.126^{a} \pm 0.003$	$222.74^{b} \pm 20.71$

ND, not detected.

Different superscript letters (a-c) indicate significant differences between samples ($P < 0.05$).

Table 3 The colour properties of the cookies

	Palm cookie	3% *CF* cookie	5% *CF* cookie
L^*	$61.23^{b} \pm 1.05$	$62.39^{b} \pm 1.63$	$55.66^{a} \pm 0.12$
a^*	$3.96^{a} \pm 0.28$	$5.14^{b} \pm 0.37$	$4.28^{a} \pm 0.28$
b^*	$23.07^{a} \pm 1.10$	$26.74^{b} \pm 1.04$	$24.42^{a} \pm 0.24$
Chroma	$23.40^{a} \pm 1.12$	$27.23^{b} \pm 1.10$	$24.79^{a} \pm 0.19$
Hue	$80.26^{b} \pm 0.28$	$79.14^{a} \pm 0.36$	$80.06^{b} \pm 0.73$
ΔL^*		1.16	−5.57
Δa^*		1.18	0.32
Δb^*		3.67	1.35
ΔE		4.03	5.74

Different superscript letters (a-b) indicate significant differences between samples ($P < 0.05$).

It is an expected result that the hardness and chewiness of the oleogels increase as the gelling agent is added to the oleogel formulation. As the amount of gel agent increases in the oleogel formulation, the interaction between chemical bonds increases and the three-dimensional network structure of the oleogel becomes stronger. As a result, the fat globules are better confined to the structure. However, the texture in the cookie formulation varies not only according to the presence of *CF* and WPI but also according to the physical, chemical and rheological properties and interactions of all other ingredients. The chewiness of the cookies may be reduced as a result of the interaction of *CF* and WPI with other ingredients (Liu & Ciftci, 2021). Also, the cohesiveness values of the dried product were between 5% *CF*-WPI and other dried products. The cohesiveness is related to internal bonds within the dried product, which is to withstand mastication before breaks. This means that 5% *CF* addition improved the internal compact structure (Golodnizky & Davidovich-Pinhas, 2020; Xie *et al*., 2023).

Oxidative stability of cookies

The study focused on examining the oxidative stability of the samples at temperatures surpassing their melting points. This approach was chosen to minimise the potential influence of the sample's structure on its oxidation stability, allowing for a direct assessment of the role played by the gelling agents. The induction periods of the cookies were found as 58.06, 53.56 and 46.42 h for the samples prepared by palm, 3% *CF*-WPI and 5% *CF*-WPI respectively. No significant changes were found between the 3% *CF*-WPI and palm cookies. These results suggested that 3% *CF*-WPI could be utilised in the production of palm alternative cookies. However, an increase in the concentration in cookie formulation caused lower induction period. The pro-oxidant effect of citrus fibre may have caused lower oxidative stability with 5% concentration. A similar result was reported by Hamidioglu *et al*. (2022) for the rice bran and candelilla wax oleogels. The results explained that the stability of oleogel depends on the properties and fatty acid composition of the oleogelator used (Kupiec *et al*., 2020; Hamidioglu *et al*., 2022). Gedikoglu *et al* found that the utilisation of citrus fibre at either 3% or 5% levels in ground beef showed a pro-oxidative influence (Hwang *et al*., 2018); they proposed that the pro-oxidant impact does not stem from hydrocarbons or wax esters. Instead, it is connected to minor constituents, notably free fatty acids. Additionally, it is possible that the pro-oxidant effect could be attributed to the existence of other unidentified compounds (Sobolev *et al*., 2022). The accelerated oxidation of oleogels might be attributed to specific minor constituents (Frolova *et al*., 2021). Similar results were reported for beeswax (Frolova *et al*., 2021).

Colour properties of the cookies

The colour properties of cookies are given in Table 3. The L value provides lighter surface area, the a value provides greenish tones and the b value provides a lower level of yellowness. The palm cookie and 3% *CF* cookie of L values showed no significant differences. The *a*, *b*, chroma and hue values of the 5% *CF* and palm cookies showed no significant differences. The ΔE values of the palm cookie and 3% *CF* cookie showed no significant differences. The colour difference in the samples could be related to the oleogel or palm oil that is used in the recipe (Yılmaz & Öğütcü, 2015).

Colour changes observed in oleogel cookies can offer valuable insights into the behaviour of chitosan–oleogels during the baking process, as well as how these colour changes are perceived by the human eye

 © 2024 The Authors. *International Journal of Food Science & Technology* published by John Wiley & Sons Ltd on behalf of Institute of Food, Science and Technology (IFSTTF).

13652621, 2024, 3, Downloaded from https://ifst.onlinelibrary.wiley.com/doi/10.1111/ijfs.16925 by Istanbul Gelisim Universitesi, Wiley Online Library on [14/02/2024]. See the Terms and Conditions (https://onlinelibrary.wiley.com/terms-and-conditions) on Wiley Online Library for rules of use; OA articles are governed by the applicable Creative Commons License

(Pathare *et al*., 2013; Brito *et al*., 2022). Notably, *CF*-WPI oleogels exhibited a yellow colour that could potentially influence colour variations in the final baked product. The act of baking prompts a significant alteration in colour, mainly due to nonenzymatic browning, primarily attributed to the Maillard reaction occurring between reducing sugars and amino acids. This reaction generates brown–yellow pigments. Notably, the baking temperature, approximately 180 °C, could have expedited chemical reactions between the citrus fibre present in the oleogels and other compounds created during baking (Brito *et al*., 2022). This interaction might have resulted in the formation of new Schiff bases, subsequently leading to the creation of fresh browning pigments (Leceta *et al*., 2013; Brito *et al*., 2022). This effect was more pronounced in cookies where *CF*-WPI-based oleogel with 5% *CF* was used, compared to those with 3% *CF*. A similar result was reported by Brito *et al*. (2022) for the 3% vanillin than the 1% vanillin in the chitosan-based oleogels in cookie formulations. Surface browning in baked goods is linked to the Maillard and caramelisation reactions (Martins *et al*., 2020; Li *et al*., 2021). The Maillard reactions encompass intricate interactions between reducing sugars and amino groups found in amino acids or proteins. In cases where amino acids are absent, sugar induces surface darkening through caramelisation (Sciarini *et al*., 2013; Li *et al*., 2021).

In terms of colour differentiation, cookies formulated with 5% *CF*-WPI displayed the highest total colour difference ($\Delta E = 5.74$) compared to palm-based cookies, followed by cookies containing oleogels with 3% *CF* ($\Delta E = 4.03$). Consequently, oleogels with 3% *CF* content yielded cookies that were visually closest to this characteristic, implying a total colour appearance most akin to cookies produced using palm oil.

Sensory properties of cookies

The sensory analysis findings of the cookies are presented in Table 4. The panellists determined that the cookies made with palm oil (4.24 ± 0.15) and cookies containing 3% *CF* oleogel (4.13 ± 0.33) had the most acceptable appearance. These were followed by cookies containing 5% *CF* (3.56 ± 0.19). Upon evaluation by the panellists, it was determined that the taste of the cookies resembled those made with palm oil and containing 3% *CF*. However, the cookies containing 5% *CF* were considered to be less strong in flavour. The panellists found no significant difference in the textural properties and colours of the cookies ($P < 0.05$). The crispness scores of cookies containing palm oil, 3% *CF* and 5% *CF* were measured as 3.65 ± 0.28, 4.04 ± 0.17 and 4.36 ± 0.22 respectively. The panellists characterised the sample with 5% *CF* oleogel as notably crispy, while the cookies with palm oil and 3% *CF* oleogel were regarded as comparable. Upon evaluating the overall acceptability of all cookies, the panellists unanimously expressed that the acceptability of all cookies was similar and of high standard. The sensory analysis findings indicated that the cookies made with oleogel-containing 3% *CF* closely resembled those made with palm oil based on the five sensory evaluations. However, the sample containing 5% *CF* could be discerned from the cookies made with palm oil. Nevertheless, it was noted that every cookie exhibited significant consumer approval and demonstrated that oleogels incorporating *CF* could serve as a substitute for palm oil.

Table 4 The sensory properties of the cookies

	Palm Cookie	3% *CF* Cookie	5% *CF* Cookie
Appearance	$4.24^{b} \pm 0.15$	$4.13^{b} \pm 0.33$	$3.56^{a} \pm 0.19$
Taste	$4.46^{b} \pm 0.22$	$4.24^{b} \pm 0.31$	$3.78^{a} \pm 0.17$
Texture	$4.07^{a} \pm 0.12$	$4.24^{a} \pm 0.14$	$4.42^{a} \pm 0.23$
Colour	$4.40^{a} \pm 0.32$	$4.23^{a} \pm 0.25$	$3.59^{a} \pm 0.29$
Crispness	$3.65^{a} \pm 0.28$	$4.04^{b} \pm 0.17$	$4.36^{b} \pm 0.22$
Overall acceptability	$4.26^{b} \pm 0.24$	$4.21^{ab} \pm 0.28$	$3.76^{b} \pm 0.26$

Different superscript letters (a-b) indicate significant differences between samples ($P < 0.05$).

Conclusion

The oleogels could be successfully produced by the emulsion-templated technique with *CF*-WPI and entrap the oil in the *CF*-WPI matrix. The structural properties of the oleogels were studied by different *CF* concentrations (1%, 2%, 35 and 5%). An increase in *CF* concentration led to a more compact, strong structure, higher oil-holding capacity and efficient entrap of the oil in gel matrix. The oleogels were successfully applied in the cookie formulation as an alternative to palm oil. The induction period and ΔE showed no significant differences meaning that *CF*-WPI oleogels could have potential in cookie formulation instead of palm oil or as saturated, trans fat replacers in foods. Future studies could be focused on the physical and chemical interaction of *CF*-WPI to improve the structural properties and widen the applicable food products as a fat replacer.

Author contributions

Ezgi Genc: Investigation; writing – original draft; visualization; data curation. **Salih Karasu:** Conceptualization; methodology; writing – review and editing; supervision. **Alican Akcicek:** Writing – original draft; visualization; methodology; conceptualization. **Omer Said Toker:** Funding acquisition; writing – review and editing.

© 2024 The Authors. *International Journal of Food Science & Technology* published by John Wiley & Sons Ltd on behalf of Institute of Food, Science and Technology (IFSTTF).

13652621, 2024, 3, Downloaded from https://ifst.onlinelibrary.wiley.com/doi/10.1111/ijfs.16925 by Istanbul Gelisim Universitesi, Wiley Online Library on [14/02/2024]. See the Terms and Conditions (https://onlinelibrary.wiley.com/terms-and-conditions) on Wiley Online Library for rules of use; OA articles are governed by the applicable Creative Commons License

Ethical statement

Ethics approval was not required for this research.

Peer review

The peer review history for this article is available at https://www.webofscience.com/api/gateway/wos/peer-review/10.1111/ijfs.16925.

Data availability statement

The data that support the findings of this study are available from the corresponding author upon reasonable request.

References

Akcicek, A., Bozkurt, F., Akgül, C. & Karasu, S. (2021). Encapsulation of olive pomace extract in rocket seed gum and chia seed gum nanoparticles: characterization, antioxidant activity and oxidative stability. *Food*, **10**, 1735.

Alizadeh, L., Abdolmaleki, K., Nayebzadeh, K. & Bahmaei, M. (2019). Characterization of sodium caseinate/Hydroxypropyl methylcellulose concentrated emulsions: effect of mixing ratio, concentration and wax addition. *International Journal of Biological Macromolecules*, **128**, 796–803.

Borriello, A., Masi, P. & Cavella, S. (2021). Novel pumpkin seed oil-based oleogels: development and physical characterization. *LWT-Food Science and Technology*, **152**, 112165.

Brito, G.B., Peixoto, V.O.D.S., Martins, M.T. *et al.* (2022). Development of chitosan-based oleogels via crosslinking with vanillin using an emulsion templated approach: structural characterization and their application as fat-replacer. *Food Structure*, **32**, 100264.

Chatsisvili, N.T., Amvrosiadis, I. & Kiosseoglou, V. (2012). Physicochemical properties of a dressing-type o/w emulsion as influenced by orange pulp fiber incorporation. *LWT- Food Science and Technology*, **46**, 335–340.

Chen, D.T., Wen, Q., Janmey, P.A., Crocker, J.C. & Yodh, A.G. (2010). Rheology of soft materials. *Annual Review of Condensed Matter Physics*, **1**, 301–322.

Chen, X.-W., Wang, J.-M., Guo, J., Wan, Z.-L., Yin, S.-W. & Yang, X.-Q. (2017). Hierarchical high internal phase emulsions and transparent oleogels stabilized by quillaja saponin-coated nanodroplets for color performance. *Food & Function*, **8**, 823–831.

Chen, X.-W., Zhang, H., Li, X.-X. & Sun, S.-D. (2023). Edible HIPE-gels and oleogels formed by synergistically combining natural triterpenoid saponin and citrus dietary fiber. *Carbohydrate Polymers*, **305**, 120499.

Davidovich-Pinhas, M., Gravelle, A.J., Barbut, S. & Marangoni, A.G. (2015). Temperature effects on the gelation of ethylcellulose oleogels. *Food Hydrocolloids*, **46**, 76–83.

Espert, M., Hernández, M.J., Sanz, T. & Salvador, A. (2022). Rheological properties of emulsion templated oleogels based on xanthan gum and different structuring agents. *Current Research in Food Science*, **5**, 564–570.

Frolova, Y. V., Sobolev, R., Sarkisyan, V., & Kochetkova, A. (2021). *Approaches to Study the Oxidative Stability of Oleogels*. IOP Conference Series: Earth and Environmental Science, IV International Scientific Conference: AGRITECH-IV-2020: Agribusiness, Environmental Engineering and Biotechnologies 18-20 November 2020, Krasnoyarsk, Russian Federation, **677**, 032045.

Giacintucci, V., Di Mattia, C.D., Sacchetti, G. *et al.* (2018). Ethylcellulose oleogels with extra virgin olive oil: the role of oil minor components on microstructure and mechanical strength. *Food Hydrocolloids*, **84**, 508–514.

Golodnizky, D. & Davidovich-Pinhas, M. (2020). The effect of the HLB value of sucrose Ester on physiochemical properties of Bigel systems. *Food*, **9**, 1857. Retrieved from https://www.mdpi.com/2304-8158/9/12/1857

Hamidioglu, I., Alenčikienė, G., Dzedulionytė, M., Zabulionė, A., Bali, A. & Šalaševičienė, A. (2022). Characterization of the quality and oxidative stability of hemp-oil-based oleogels as an animal fat substitute for meat patties. *Food*, **11**, 4030.

Hong, X., Zhao, Q., Chen, J., Ye, T., Fan, L. & Li, J. (2022). Fabrication and characterization of oleogels and temperature-responsive water-in-oil emulsions based on candelilla (Euphorbia cerifera) wax. *Food Chemistry*, **397**, 133677.

Huang, L., Cai, Y., Fang, D. *et al.* (2023). Formation and characterization of oleogels derived from emulsions: evaluation of polysaccharide ratio and emulsification method. *Food Hydrocolloids*, **142**, 108844.

Hwang, H.S., Fhaner, M., Winkler-Moser, J.K. & Liu, S.X. (2018). Oxidation of fish oil oleogels formed by natural waxes in comparison with bulk oil. *European Journal of Lipid Science and Technology*, **120**, 1700378.

Jadhav, H.B., Pratap, A.P., Gogate, P.R. & Annapure, U.S. (2022). Ultrasound-assisted synthesis of highly stable MCT based oleogel and evaluation of its baking performance. *Applied Food Research*, **2**, 100156.

Jiang, Y., Liu, L., Wang, B. *et al.* (2018). Cellulose-rich oleogels prepared with an emulsion-templated approach. *Food Hydrocolloids*, **77**, 460–464.

Kupiec, M., Zbikowska, A., Marciniak-Lukasiak, K. & Kowalska, M. (2020). Rapeseed oil in new application: assessment of structure of oleogels based on their physicochemical properties and microscopic observations. *Agriculture*, **10**, 211.

Laredo, T., Barbut, S. & Marangoni, A.G. (2011). Molecular interactions of polymer oleogelation. *Soft Matter*, **7**, 2734.

Leceta, I., Guerrero, P. & De La Caba, K. (2013). Functional properties of chitosan-based films. *Carbohydrate Polymers*, **93**, 339–346.

Li, S., Wu, G., Li, X., Jin, Q., Wang, X. & Zhang, H. (2021). Roles of gelator type and gelation technology on texture and sensory properties of cookies prepared with oleogels. *Food Chemistry*, **356**, 129667.

Li, J., Xi, Y., Wu, L. & Zhang, H. (2023a). Preparation, characterization and in vitro digestion of bamboo shoot protein/soybean protein isolate based-oleogels by emulsion-templated approach. *Food Hydrocolloids*, **136**, 108310.

The focus of this work is to analyse and describe the properties and composition of oleogels that are formed using emulsion templates. The focus of our investigation is the synthesis of oleogel *via* emulsion templating.

Li, Y., Zhang, C., Hu, B. *et al.* (2023b). Formation and application of edible oleogels prepared by dispersing soy fiber particles in oil phase. *Food Research International*, **164**, 112369.

This study is related to fibre-based oleogels characterisation. This study is a current study to compare our results.

Liu, L. & Ciftci, O.N. (2021). Effects of high oil compositions and printing parameters on food paste properties and printability in a 3D printing food processing model. *Journal of Food Engineering*, **288**, 110135.

Ma, Y., Ye, F., Chen, J. *et al.* (2023). The microstructure and gel properties of linseed oil and soy protein isolate based-oleogel constructed with highland barley β-glucan and its application in luncheon meat. *Food Hydrocolloids*, **140**, 108666.

Manzoor, S., Masoodi, F., Naqash, F. & Rashid, R. (2022). Oleogels: promising alternatives to solid fats for food applications. *Food Hydrocolloids for Health*, **2**, 100058.

 © 2024 The Authors. *International Journal of Food Science & Technology* published by John Wiley & Sons Ltd on behalf of Institute of Food, Science and Technology (IFSTTF).

13652621, 2024, 3, Downloaded from https://ifst.onlinelibrary.wiley.com/doi/10.1111/ijfs.16925 by Istanbul Gelisim Universitesi, Wiley Online Library on [14/02/2024]. See the Terms and Conditions (https://onlinelibrary.wiley.com/terms-and-conditions) on Wiley Online Library for rules of use; OA articles are governed by the applicable Creative Commons License

Martins, A.J., Vicente, A.A., Pastrana, L.M. & Cerqueira, M.A. (2020). Oleogels for development of health-promoting food products. *Food Science and Human Wellness*, **9**, 31–39.

Meng, Z., Qi, K., Guo, Y., Wang, Y. & Liu, Y. (2018). Macro-micro structure characterization and molecular properties of emulsion-templated polysaccharide oleogels. *Food Hydrocolloids*, **77**, 17–29.

Ozulku, G., Yildirim, R.M., Toker, O.S., Karasu, S. & Durak, M.Z. (2017). Rapid detection of adulteration of cold pressed sesame oil adultered with hazelnut, canola, and sunflower oils using ATR-FTIR spectroscopy combined with chemometric. *Food Control*, **82**, 212–216.

Pathare, P.B., Opara, U.L. & Al-Said, F.A.-J.. (2013). Colour measurement and analysis in fresh and processed foods: A review. *Food and Bioprocess Technology*, **6**, 36–60.

Plazzotta, S., Calligaris, S. & Manzocco, L. (2020). Structural characterization of oleogels from whey protein aerogel particles. *Food Research International*, **132**, 109099.

Qiu, C., Huang, Y., Li, A., Ma, D. & Wang, Y. (2018). Fabrication and characterization of oleogel stabilized by gelatin-polyphenol-polysaccharides nanocomplexes. *Journal of Agricultural and Food Chemistry*, **66**, 13243–13252.

This study was used to produce emulsion template oleogels.

Rao, M.A. (2010). *Rheology of Fluid and Semisolid Foods: Principles and Applications*. Boston, MA, USA: Springer Science & Business Media.

Ruan, Q., Yang, X., Zeng, L. & Qi, J. (2019). Physical and tribological properties of high internal phase emulsions based on citrus fibers and corn peptides. *Food Hydrocolloids*, **95**, 53–61.

Sciarini, L.S., Van Bockstaele, F., Nusantoro, B., Perez, G.T. & Dewettinck, K.. (2013). Properties of sugar-snap cookies as influenced by lauric-based shortenings. *Journal of Cereal Science*, **58**(2), 234–240.

Shuai, X., McClements, D.J., Geng, Q. *et al*. (2023). Macadamia oil-based oleogels as cocoa butter alternatives: physical properties, oxidative stability, lipolysis, and application. *Food Research International*, **172**, 113098.

da Silva, T.L.T., Arellano, D.B. & Martini, S. (2019). Interactions between candelilla wax and saturated triacylglycerols in oleogels. *Food Research International*, **121**, 900–909.

Sobolev, R., Frolova, Y., Sarkisyan, V., Makarenko, M. & Kochetkova, A. (2022). Effect of beeswax and combinations of its fractions on the oxidative stability of oleogels. *Food Bioscience*, **48**, 101744.

Song, Y.-t., Qi, J.-r., Yang, X.-q., Liao, J.-s., Liu, Z.-w. & Ruan, C.-w. (2022). Hydrophobic surface modification of citrus fiber using octenyl succinic anhydride (OSA): preparation, characterization and emulsifying properties. *Food Hydrocolloids*, **132**, 107832.

Tavernier, I., Patel, A.R., Van der Meeren, P. & Dewettinck, K. (2017). Emulsion-templated liquid oil structuring with soy protein and soy protein: κ-carrageenan complexes. *Food Hydrocolloids*, **65**, 107–120.

Wijaya, W., Sun, Q.-Q., Vermeir, L., Dewettinck, K., Patel, A.R. & Van der Meeren, P. (2019). pH and protein to polysaccharide ratio control the structural properties and viscoelastic network of HIPE-templated biopolymeric oleogels. *Food Structure*, **21**, 100112.

Xie, F., Ren, X., Zhu, Z. *et al*. (2023). Tamarind seed polysaccharide-assisted fabrication of stable emulsion-based oleogel structured with gelatin: preparation, interaction, characterization, and application. *Food Hydrocolloids*, **142**, 108761.

Xu, C., Zhan, W., Tang, X., Mo, F., Fu, L. & Lin, B. (2018). Self-healing chitosan/vanillin hydrogels based on Schiff-base bond/hydrogen bond hybrid linkages. *Polymer Testing*, **66**, 155–163.

Xu, Y., Sun, H., Lv, J., Wang, Y., Zhang, Y. & Wang, F. (2023). Effects of polysaccharide thickening agent on the preparation of walnut oil oleogels based on methylcellulose: characterization and delivery of curcumin. *International Journal of Biological Macromolecules*, **232**, 123291.

Yılmaz, E. & Öğütcü, M. (2015). The texture, sensory properties and stability of cookies prepared with wax oleogels. *Food & Function*, **6**, 1194–1204.

This study is related to oleogel-based cookie production. We use this study to compare our results.

Yoo, B. & Rao, M. (1996). Creep and dynamic rheological behavior of tomato concentrates: effect of concentration and finisher screen size. *Journal of Texture Studies*, **27**, 451–459.

Zhao, W., Wei, Z., Xue, C. & Meng, Y. (2023). Development of food-grade oleogel via the aerogel-templated method: oxidation stability, astaxanthin delivery and emulsifying application. *Food Hydrocolloids*, **134**, 108058.

© 2024 The Authors. *International Journal of Food Science & Technology* published by John Wiley & Sons Ltd on behalf of Institute of Food, Science and Technology (IFSTTF).

13652621, 2024, 3, Downloaded from https://ifst.onlinelibrary.wiley.com/doi/10.1111/ijfs.16925 by Istanbul Gelisim Universitesi, Wiley Online Library on [14/02/2024]. See the Terms and Conditions (https://onlinelibrary.wiley.com/terms-and-conditions) on Wiley Online Library for rules of use; OA articles are governed by the applicable Creative Commons License